

Closed formula for the transport of micro- nano-particle across model porous media

Paolo Magaretti^{1,*} and Jens Harting^{1,2}

¹*Helmholtz Institute Erlangen-Nürnberg for Renewable Energy (IEK-11), Forschungszentrum Jülich, Erlangen, Germany*

²*Department of Applied Physics, Eindhoven University of Technology, Eindhoven, The Netherlands*

In the last decade the Fick-Jacobs approximation has been exploited to capture the transport across constrictions. Here, we review the derivation of the Fick-Jacobs equation with particular emphasis on its linear response regime. We show that for fore-aft symmetric channels the flux of non-interacting systems is fully captured by its linear response regime. For this case we derive a very simple formula that captures the correct trends and that can be exploited as a simple tool to design experiments or simulations. Finally, we show that higher order corrections in the flux may appear for non-symmetric channels.

I. INTRODUCTION

It is common to experience long queues form when a constriction occurs on a highway [1, 2]. Such an (unlucky) phenomenon is clearly the result of the “local” confinement: due to the constriction, vehicles slow down hence reducing the local “mass” flux as compared to the clear part of the highway. Such a local reduction of the mass flow causes the onset of the annoying queues that every now and then we experience. This phenomenon does not occur only on highways. It becomes a major issue close to emergency exits in the case of panic [3]. The very same dynamics occurs also at smaller scales and for simpler systems. For example, it is common experience that it is difficult to extract pills from a container if the opening is too small. Here, pills tend to “clog” i.e., to form stable structures close to the opening of the container that prevent pills from going out. The very similar dynamics occurs in silos containing crops [4], in erosion [5], in suspensions of hard and soft particles [6–8], in herds of sheep [9], in the onset of panic in ants [10], and even humans [11].

The effect of confinement does not have to be unpleasant, as it is for traffic jams, or inconvenient, as it is for clogging of silos. Vice versa, tuning the shape of the confining media can be an intriguing and novel way to control the dynamics of the confined system. For example, microfluidic devices exploit variations of the section of the micro channels they are made of to control the dynamics of fluid and to induce the formation of droplets [12–15]. Similarly, Tunable Resistive Pulse Sensing (TRPS) techniques exploit micro- nano-pores to analyze small particles ranging from a few tens of nanometers up to micrometric scale [16]. In particular, TRPS has been used to direct detect antibody-antigen binding [17], to measure electrophoretic mobility of colloidal particles [18], to perform single-molecule detection [19] and to measure the zeta-potential of nanometric particles [20]. Alternatively, Chromatography techniques have been developed to separate micro- or nano-particles depending on both their size as well as their surface properties [21–24]. Finally, at even smaller scales, nanopores have been designed to sequence DNA molecules [25].

Transport in confinement is not relevant only for particle detection/analysis. Indeed, the flow of fluids across a porous medium is crucial in diverse scenarios. For example, oil recovery industries have put much effort into developing techniques to maximize the extraction of oil from the rock matrix it is embedded in [26, 27]. Similarly, understanding the dependence of the flow of water on the porosity of the soil is crucial in environmental sciences [28]. Moreover, diverse technologies related to the energy transition such as blue-energy [29], hydrogen technology [30, 31], electrolyzers and fuel cells [32, 33], or CO_2 segregation [34] rely on the transport of (charged) chemical species across nanoporous materials.

Finally, several biological systems are controlled by the transport of confined complex fluids. For example, neuronal transmission relies on the transport of neuro-receptors among neurons and to their specific binding sites [35]. Moreover, cell regulation relies on the proper tuning of the concentrations of electrolytes inside the cell. Such a regulation occurs via dedicated pores and channels whose shape makes them very sensitive to specific ions [36–40] and RNA is transported across the nuclear membrane [41–43]. Moreover, the lymphatic and circulatory systems in mammals rely on the transport of quite heterogeneous suspensions composed of a variety of components, spanning from the nanometric size of ions up to the micrometric size of red blood cells, across varying-section elastic pipes [7, 44–46]. Finally, the survival of plants relies, at large scales, on the proper circulation of liquid (sap) along the trunk [47] and at short scales on the cytoplasmic streaming within the cells [48].

*Corresponding Author: p.magaretti@fz-juelich.de

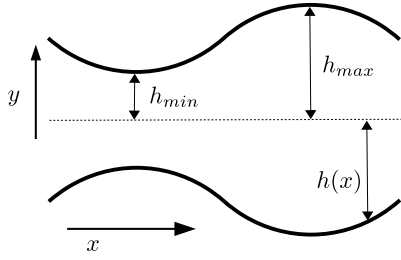


FIG. 1: Cartoon of the varying-section channel.

All the above mentioned systems rely or depend on the dynamics under confinement. Therefore, understanding the dynamics and transport properties of confined complex systems such as ions, molecules, polymers, colloidal particles, and suspensions is of primary importance for the understanding of a wide spectrum of phenomena and for the development of technological applications. Even more, identifying the relevant parameters controlling key features, like transport or phase transitions, will open a new route for controlling the dynamics of confined systems upon tuning the geometry of the confining media.

Up to now, there has been no systematic study of the dependence of the dynamics of confined systems upon changing the shape of the confining walls. The main reason is the large effort that such a study requires. Indeed, *experimentally* tuning the shape of a pore is a tremendous task since, if possible at all, it requires to synthesize every time a new item from scratch. On the *theoretical* side, studying the dynamics and the transport of confined systems is a tremendous task since it requires to capture several length, time and energy scales. In fact, the length scales range from the nanometric scale, typical for ions and for van der Waals interactions to the micrometric scale of colloids, polymers and macromolecules up to the millimeters/centimeters scale of microfluidic devices. Concerning time scales, the spectrum spans the diffusion time of small particles and ions over their size $\sim \mu\text{sec}$ up to the long time scales typical of transport $\sim \text{sec}$. Concerning energy scales, they range from thermal energy $k_B T$ ($\sim 10^{-21} \text{J}$) up to van der Waals and electrostatic interactions whose magnitude can be of several $k_B T$. On the top of these “direct” interactions also the effective interactions induced by the confinement should be accounted for. For example, squeezing a deformable object, like a polymer or a vesicle, through a constriction can require quite an amount of energy that can easily reach the order of $100 - 1000 k_B T$. Given such a complexity, one typically would rely on numerical techniques such as molecular dynamics. However, the wide range of interactions (Van der Waals, electrostatic..) jointly with the wide range of time and length scales imposes to put forward numerical approaches capable of properly resolving the smallest length, time and energy scales. At the same time, such an approach should also resolve the large length, time and energy scales. Accordingly, the numerical route becomes quite demanding from the perspective of the computational time.

Since both experimental and numerical routes are quite expensive, an approximated analytical route based on some controllable expansions may become appealing. Intriguingly, it is possible to obtain simple analytical models that capture some features of the dynamics of confined systems. The key idea, is to “project” the dynamics of the system onto some relevant coordinate (in chemistry sometimes called “reaction coordinate”) and then to study the dynamics of these few (typically one) degrees of freedom. For example, in the case of polymer translocation across pores, the most important observable is the time the polymer takes to cross from one side to the other of the pore. Therefore, the relevant degree of freedom is the position of the center of mass of the polymer whereas the degrees of freedom associated with the position of the monomers can be integrated out.

In this contribution, we briefly review the derivation of the Fick-Jacobs approximation [49–56] and its use in studying transport across corrugated pores and channels. The Fick-Jacobs approximation has been shown to be applicable to the transport of ions [57–61], colloids [62–66], rods [67], polymers [68–70], and more recently even active systems [71–73], chemical reactors [74] and pattern-forming systems [75].

In the following we re-derive the Fick-Jacobs approximation with particular emphasis on the regime in which the current is proportional to the applied force. In such a regime, it is possible to derive a closed formula that accounts for the dependence of the flux on the geometry of the channel. Interestingly, our derivation naturally highlights a few relations between the underlying Smoluchowski equation and the linear response theory. Even though this work is motivated by the transport in confined pores and channels, the results we derive are valid for all $1D$ systems (independently of the physical origin of the effective potential) in the dilute regime (for which mutual interactions can be neglected) and whose dynamics is governed by the Smoluchowski equation (i.e. in the overdamped regime).

II. MODEL

In the following we are interested in the transport of a single colloidal particle confined in an axially symmetric channel characterized by its half section (see Fig. 1 for a sketch of the system)

$$h(x) = h_0 + h_1 \cos\left(2\pi\frac{x}{L}\right). \quad (1)$$

The time evolution of the probability density is governed by the Smoluchowski equation

$$\dot{\rho}(\mathbf{r}, t) = \nabla \cdot [D\nabla\rho(\mathbf{r}, t) + D\beta\rho(\mathbf{r}, t)\nabla W(\mathbf{r})], \quad (2)$$

where D is the diffusion coefficient, $\beta^{-1} = k_B T$ is the inverse thermal energy, k_B the Boltzmann constant, T the absolute temperature and

$$W(\mathbf{r}) = \begin{cases} \phi(\mathbf{r}) & |r| < h(x) \\ \infty & \text{else} \end{cases} \quad (3)$$

is the effective potential responsible for both confining the particle within the channel and for additional soft interactions, $\phi(\mathbf{r})$ with the channel walls. For smoothly-varying channel cross-sections, $\partial_x h(x) \ll 1$, it is possible to factorize the probability density [49, 50, 53–56]

$$\rho(\mathbf{r}, t) = p(x, t) \frac{e^{-\beta W(\mathbf{r})}}{e^{-\beta A(x)}}, \quad (4)$$

where

$$A(x) = -k_B T \ln \left[\frac{1}{\pi h_0^2} \int_{-\infty}^{\infty} e^{-\beta W(\mathbf{r})} r dr \right] \quad (5)$$

is the local free energy [76]. Moreover, integrating along the radial direction leads to

$$\dot{p}(x, t) = \partial_x [D\partial_x p(x, t) + D\beta p(x, t)\partial_x A(x)]. \quad (6)$$

Such a procedure is called *Fick-Jacobs approximation* [49, 50, 56]. Its regime of validity has been assessed by several groups [51, 52, 54, 62, 77–82]. In particular, it has been shown that the quantitative reliability of the Fick-Jacobs approximation can be enhanced by introducing a position dependent diffusion coefficient [51, 52, 54, 62, 77–82], $D(x)$, hence leading to the set of equations

$$\dot{p}(x, t) = -\partial_x J(x, t) \quad (7)$$

$$\frac{J}{D(x)} = -\partial_x p(x) - \beta p(x)\partial_x A(x). \quad (8)$$

Eq. (8) is completed with the boundary conditions

$$p(-L) = p(L) \quad (9)$$

$$\int_{-L}^L p(x) dx = 1. \quad (10)$$

We decompose the effective force $-\partial_x A(x)$ as the net force

$$f = -\frac{1}{2L} \int_{-L}^L \partial_x A(x) dx = -\frac{\Delta A}{2L} \quad (11)$$

and

$$A_{eq}(x) = A(x) + fx. \quad (12)$$

f accounts for the net force responsible of the flux and $A_{eq}(x)$ accounts for all the other conservative forces that will not give rise to any flux. In the following, we expand both the flux, J , and the density, p , about the equilibrium case:

$$J = J_0 + J_1 + J_2 + \dots \quad (13)$$

$$p(x) = p_0(x) + p_1(x) + p_2(x) + \dots \quad (14)$$

Note that due to Eq. (10) at zeroth order we have

$$\int_{-L}^L p_0(x) dx = 1. \quad (15)$$

This implies

$$\int_{-L}^L p_n(x) dx = 0 \quad \forall n \neq 0 \quad (16)$$

Accordingly, at order zero we have

$$p_0(x) = \tilde{p} e^{-\beta A_{eq}(x)} \quad (17)$$

$$J_0 = 0 \quad (18)$$

$$\tilde{p} = \frac{1}{\int_{-L}^L e^{-\beta A_{eq}(x)} dx}. \quad (19)$$

At the generic n -th order we have

$$\frac{J_n}{D(x)} = -\partial_x p_n(x) - \beta p_n(x) \partial_x A_{eq}(x) + \beta p_{n-1}(x) f, \quad (20)$$

the solution of which reads

$$p_n(x) = e^{-\beta A_{eq}(x)} \left[\int_{-L}^x \left[\beta p_{n-1}(y) f - \frac{J_n}{D(y)} \right] e^{\beta A_{eq}(y)} dy + \Pi_n \right]. \quad (21)$$

Here, J_n and Π_n are integration constants. Imposing the periodic boundary conditions, $p_n(-L) = p_n(L)$, and recalling that $A_{eq}(-L) = A_{eq}(L)$ leads to

$$\int_{-L}^L \left(\frac{J_n}{D(y)} - \beta p_{n-1}(y) f \right) e^{\beta A_{eq}(y)} dy = 0, \quad (22)$$

with

$$J_n = \beta f \frac{\int_{-L}^L p_{n-1}(y) e^{\beta A_{eq}(y)} dy}{\int_{-L}^L \frac{e^{\beta A_{eq}(y)}}{D(y)} dy} = \beta f \tilde{p} \frac{\int_{-L}^L \frac{p_{n-1}(y)}{p_0(y)} dy}{\int_{-L}^L \frac{e^{\beta A_{eq}(y)}}{D(y)} dy}. \quad (23)$$

In the last step we used Eq. (17). Finally, Π_n is determined by imposing Eqs. (15), (16)

$$\Pi_n = -\tilde{p} \int_{-L}^L e^{-\beta A_{eq}(x)} \int_{-L}^x \left[\beta p_{n-1}(y) f - \frac{J_n}{D(y)} \right] e^{\beta A_{eq}(y)} dy dx. \quad (24)$$

At leading order in the force, Eqs. (21) (23) read

$$p_1(x) = e^{-\beta A_{eq}(x)} \left[\beta f \tilde{p} (x+L) - J_1 \int_{-L}^x \frac{e^{\beta A_{eq}(y)}}{D(y)} dy \right], \quad (25)$$

$$J_1 = \frac{2\beta f L}{\int_{-L}^L e^{-\beta A_{eq}(x)} dx \int_{-L}^L \frac{e^{\beta A_{eq}(x)}}{D(x)} dx}. \quad (26)$$

Interestingly, from Eq. (26), it is possible to identify a force-independent channel permeability

$$\chi = \frac{2\beta L}{\int_{-L}^L e^{-\beta A_{eq}(x)} dx \int_{-L}^L \frac{e^{\beta A_{eq}(x)}}{D(x)} dx}. \quad (27)$$

As expected, Eq. (27) agrees with the derivation of the effective diffusion coefficient for a particle at equilibrium and in the presence of entropic barriers [83, 84]. This is in agreement with the linear response theory within which the transport coefficients that determine the flux under external forces can be determined from equilibrium properties.

Some general remarks can be derived in the case of fore-aft symmetric channels, for which $A_{eq}(x) = A_{eq}(-x)$, and diffusivities, $D(x) = D(-x)$. For such cases, the magnitude of the flux should depend solely on the magnitude of the force and not on its sign. This implies that

$$J_{2n} = 0, \quad \forall n > 0. \quad (28)$$

In order to proceed, we recall that, for fore-aft symmetric $f(x)$ and $g(x)$, the following equality holds:

$$\int_{-L}^L g(x) \int_{-L}^x f(y) dy dx = \frac{1}{2} \int_{-L}^L f(x) dx \int_{-L}^L g(x) dx \quad (29)$$

Enforcing the condition in Eq. (28) into Eq. (23) and using the last expression leads to

$$\Pi_n = 0, \quad \forall n > 0. \quad (30)$$

and, substituting again into Eq. (23) eventually leads to

$$J_n = 0, \quad \forall n \geq 1. \quad (31)$$

Interestingly, we note that even though $\Pi_{n>0} = 0$ and $J_{n>1} = 0$ the density profile is still sensitive to higher order corrections in the force, i.e. in general $p_n \neq 0$. According to this analysis, Eq. (26) is not just the linear contributions to the flux rather it provides the exact expressions at every order in the external force. The outcome of this analysis is indeed intuitive since it states that for non-interacting systems confined within fore-aft symmetric channels non-linear effects are absent. The same results are indeed valid for any 1D problem with such a symmetry.

In contrast, if neither the potential, $A(x)$, nor the diffusion profile, $D(x)$, have a defined parity, then the left-right symmetry is broken, Eq. (28) does not hold anymore, and indeed a diode effect may set for sufficiently large external forces. We can assess the dependence of the diode effect on the geometry of the channel by calculating

$$J_2 = \beta f \frac{\int_{-L}^L \int_{-L}^x \beta \tilde{p} f - \frac{J_1}{D(y)} e^{\beta A_{eq}(y)} dy + \Pi_1 dx}{\int_{-L}^L \frac{e^{\beta A_{eq}(y)}}{D(y)} dy}. \quad (32)$$

Using

$$\Gamma(x) = \int_{-L}^x \frac{e^{\beta A_{eq}(y)}}{D(y)} dy \quad (33)$$

and the definition of J_1 we obtain

$$J_2 = \frac{\beta f}{\Gamma(L)} \int_{-L}^L \beta \tilde{p} f(x+L) - 2\beta \tilde{p} f L \frac{\Gamma(x)}{\Gamma(L)} + \Pi_1 dx. \quad (34)$$

Finally, using the definition of Π_1 we obtain

$$J_2 = \frac{(\beta f L)^2 \tilde{p}}{\Gamma(L)} \frac{1}{L} \int_{-L}^L \left[\left(\frac{x}{L} + 1 \right) - 2 \frac{\Gamma(x)}{\Gamma(L)} \right] \left[1 - e^{-\beta A_{eq}(x)} \right] dx. \quad (35)$$

A. Transport across free energy barriers

In the case of transport of point-like particles across 3D varying-section channels with axial symmetry the effective potential reads

$$A_{eq}^{(id)}(x) = -2k_B T \ln \left[\frac{h(x)}{h_0} \right], \quad (36)$$

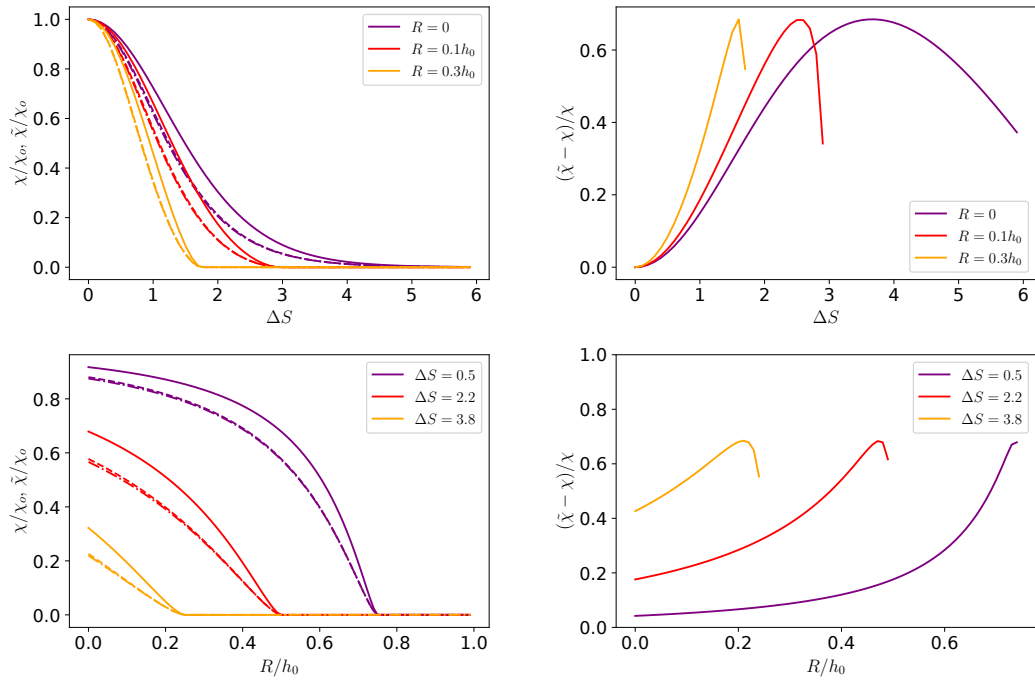


FIG. 2: Transport across porous media. Upper left: permeability, χ , as obtained from Eq. (46) (solid lines), Eq. (26) with constant diffusion coefficient (dashed lines) and Eq. (26) with a diffusion coefficient as given by Eq. (40) (dashed-dotted lines) normalized by the one across a constant-section channel $\chi_o = D\beta/4L$, as function of the geometry of the channel $\Delta S = \ln \frac{h_o+h_1}{h_o-h_1} = \ln \frac{h_{max}}{h_{min}}$ for different values of the particle radius. Bottom: permeability, χ , normalized by the one across a constant-section channel $\chi_o = D\beta/4L$, as function of the radius of the particle, R , normalized by the average channel width, h_o , for different channel geometries captured by ΔS . Upper right: ratio of $\tilde{\chi}$ over χ normalized by χ for the data sets shown in the left panel. Bottom right: ratio of $\tilde{\chi}$ over χ normalized by χ for the data sets shown in the left panel.

where $h(x)$ is the local half-section of the channel and h_o its average value (see Fig.1). Accordingly, Eq. (26) reads

$$J_{id} = \frac{2\beta f L}{\int_{-L}^L \frac{h^2(x)}{h_o^2} dx \int_{-L}^L \frac{h_o^2}{h^2(x)D(x)} dx}. \quad (37)$$

In the case of micro- or nano-particles that undergo solely excluded volume interactions with the channel walls, the effective channel half-section becomes $h(x) - R$ where R is the particle size and we obtain

$$A_{eq}^{(pcl)}(x) = -2k_B T \ln \left[\frac{h(x) - R}{h_o} \right], \quad (38)$$

which leads to

$$J_{pcl} = \frac{2\beta f L}{\int_{-L}^L \frac{(h(x)-R)^2}{h_o^2} dx \int_{-L}^L \frac{h_o^2}{(h(x)-R)^2 D(x)} dx}. \quad (39)$$

We recall that $R < h_o - h_1$ for the particle to be able to cross the channel. Finally, several groups have shown that the Fick-Jacobs approximation can be improved by assuming a position-dependent diffusion coefficient [49, 50, 53, 54, 79–82]. Nowadays, there is general agreement that the approximated formula for the diffusion coefficient reads [50] (or is in practice equivalent to)

$$D(x) = \frac{D_o}{\sqrt{1 + (\partial_x h(x))^2}}. \quad (40)$$

B. Piece-wise linear potential and homogeneous diffusion coefficient

In order to get analytical insight it can be useful to approximate the effective potential $A(x)$ by

$$A_{eq}(x) = -\frac{\Delta A_{eq}}{L}|x|, \quad (41)$$

where

$$\Delta A_{eq} = A_{eq}^{max} - A_{eq}^{min} \quad (42)$$

is the piece-wise linear difference between the maximum and minimum values of A_{eq} . Moreover, if we assume that the diffusion coefficient is homogeneous

$$D(x) = D_0 \quad (43)$$

we get

$$\int_{-L}^L e^{\beta A_{eq}(x)} dx = \frac{2L}{\beta \Delta A_{eq}} (1 - e^{-\beta \Delta A_{eq}}) \quad (44)$$

$$\int_{-L}^L e^{-\beta A_{eq}(x)} dx = \frac{2L}{\beta \Delta A_{eq}} (e^{\beta \Delta A_{eq}} - 1) \quad (45)$$

and finally by substituting the last expressions into Eq. (27) we obtain an approximated expression for the permeability

$$\tilde{\chi} = \frac{D\beta}{4L} \frac{(\beta \Delta A_{eq})^2}{\cosh(\beta \Delta A_{eq}) - 1}. \quad (46)$$

Interestingly, Eq. (46) shows that χ is an even function of ΔA_{eq} . This implies that the transport is insensitive upon flipping the sign of the free energy barrier ΔA . Finally, Eq.(46) shows that χ decays exponentially with $\beta \Delta A_{eq}$.

III. DISCUSSION

The reliability of the Fick-Jacobs approximation, namely Eq.(26), has been addressed for point-like particles and it has shown good quantitative agreement for forces up to $\beta f L \simeq 10$ [78]. However, Eq. (26) still requires to numerically compute integrals, whereas Eq. (46) provides a direct (yet approximated) dependence of $\tilde{\chi}$ on ΔA . Therefore, it is important to address the reliability of Eq. (46) as compared to the full solution Eq. (26). Indeed, all the panels of Fig. 2 show that the permeability calculated with the piece-wise linear model, Eq. (46), shows some discrepancies as compared to the full expression give in Eq. (26). In particular, as shown in Fig. 2 for the case under consideration ($h_0/L = 0.1$) the corrections due to the inhomogeneous diffusion (dashed-dotted lines) are indistinguishable from those with constant diffusion coefficient (dashed lines) and hence they do not improve the approximation. On the other hand Fig. 2 shows that the simple formula in Eq. (46) is sufficient to properly capture the trends and indeed can be used to estimate the transport of colloidal particle across porous media. Interestingly, concerning the magnitude of χ , the bottom panels of Fig. 2 show that the channel permeability decreases upon increasing the particle size. Interestingly, the decrease is almost linear for larger corrugations of the channel (larger values of ΔS) whereas for smaller values of the corrugation it plateaus at smaller values of R .

Finally, we discuss the dependence of $\tilde{\chi}$ in $\beta \Delta A$ as per Eq. (46). As shown in Fig. (3), $\tilde{\chi}$ has a maximum for $\beta \Delta A = 0$ and then it decays exponentially for larger values of $\beta \Delta A$. Interestingly, $\tilde{\chi}$ attains values close to unity up to $\beta \Delta A \simeq 5$, i.e. for a free energy barrier much larger than the thermal energy.

The fact that Eq. (46) depends solely on ΔA allows one to estimate the transport also in situations in which the particles may have some soft interactions with the walls, like electrostatic interactions. In that case the free energy barrier will depend not only on the size of the particle and on the geometry of the channel but also on the charge of both the particle and the walls of the channels [58, 76]. Moreover, Eq. (46) allows also to predict the transport of soft or deformable objects, like proteins or polymers [68, 69, 85].

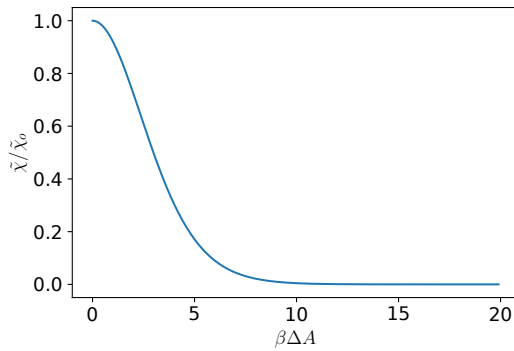


FIG. 3: Dependence of the approximated channel permeability, $\tilde{\chi}$, (as defined in Eq. (46)) normalized by that of a constant section channel, χ_o as function of the amplitude of the dimensionless free energy barrier $\beta\Delta A$ which encodes the physical properties of the confined system.

IV. CONCLUSIONS

We have derived closed formulas for the transport within linear response theory as well as for higher order corrections. In particular, we have shown that for the case of non-interacting systems confined in fore-aft symmetric channels the higher order corrections in both the flux and in the density are identically zero. Hence, for fore-aft symmetric channels, the full expression for the flux is indeed the one obtained within the linear response regime. Accordingly, the channel permeability derived within linear response, Eq. (27), is related to the well known expression of the effective diffusion coefficient reported in the literature [83, 84]. Moreover, we have shown that, within the linear response, the formula for the permeability χ , Eq. (27), can be further simplified by approximating the local free energy by piece-wise linear potential (Eq. (41)) to obtain Eq. (46), whose overall drop is determined by the values of the free energy at the bottleneck and at the waist of the channel. We have shown that such an approximation provides the correct trends and it is reliable within $\simeq \pm 50\%$ as shown in the right panels of Fig. 2. This feature is crucial since Eq. (46) can be easily computed and it is valid for all soft-interactions between the particle and the channel walls.

Acknowledgments

We thank I. Pagonabarraga and J. Schmid for insightful discussions and acknowledge funding by the Deutsche Forschungsgemeinschaft (DFG, German Research Foundation) – Project-ID 416229255 – SFB 1411 and Project-ID 431791331 – SFB 1452.

-
- [1] M. J. Lighthill and G. B. Whitham, Proceedings of the Royal Society of London. Series A. Mathematical and Physical Sciences **229**, 317 (1955).
 - [2] C. Wang, M. A. Quddus, and S. G. Ison, Safety Science **57**, 264 (2013), ISSN 0925-7535.
 - [3] H. Vermuyten, J. Belian, L. De Boeck, G. Reniers, and T. Wauters, Safety Science **87**, 167 (2016), ISSN 0925-7535.
 - [4] H. Y. Jeong, S.-C. Jun, J.-Y. Cheon, and M. Park, Geosciences Journal **22**, 667 (2018).
 - [5] R. Jäger, M. Mendoza, and H. J. Herrmann, Phys. Rev. Fluids **3**, 074302 (2018).
 - [6] A. Marin, H. Lhuissier, M. Rossi, and C. J. Kähler, Phys. Rev. E **97**, 021102 (2018).
 - [7] R. Kusters, T. van der Heijden, B. Kaoui, J. Harting, and C. Storm, Phys. Rev. E **90**, 033006 (2014).
 - [8] C. Bielinski, O. Aouane, J. Harting, and B. Kaoui, Phys. Rev. E **104**, 065101 (2021).
 - [9] A. Garcimartín, J. M. Pastor, L. M. Ferrer, J. J. Ramos, C. Martín-Gómez, and I. Zuriguel, Phys. Rev. E **91**, 022808 (2015).
 - [10] E. Altshuler, O. Ramos, Y. Nuñez, J. Fernandez, A. Batista-Leyva, and C. Noda, The American Naturalist **166**, 643 (2005).
 - [11] I. Zuriguel, I. Echevería, D. Maza, R. C. H. anésar Martín-Gómez, and A. Garcimartín, Safety Science **121**, 394 (2020), ISSN 0925-7535, URL <http://www.sciencedirect.com/science/article/pii/S0925753519310203>.
 - [12] T. M. Squires and S. R. Quake, Rev. Mod. Phys. **77**, 977 (2005).
 - [13] E. Dressaire and A. Sauret, Soft Matter **13**, 37 (2017).
 - [14] K. Doufène, C. Tourné-Péteilh, P. Etienne, and A. Aubert-Pouëssel, Langmuir **35**, 12597 (2019).

- [15] N. Convery and N. Gadegaard, *Micro and Nano Engineering* **2**, 76 (2019), ISSN 2590-0072, URL <http://www.sciencedirect.com/science/article/pii/S2590007219300036>.
- [16] E. Weatherall and G. R. Willmott, *Analyst* **140**, 3318 (2015).
- [17] O. A. Saleh and L. L. Sohn, *Proc. Natl. Acad. Sci. U. S. A.* **100**, 820 (2003).
- [18] T. Ito, L. Sun, M. A. Bevan, and R. M. Crooks, *Langmuir* **20**, 6940 (2004).
- [19] E. A. Heins, Z. S. Siwy, L. A. Baker, and R. C. Martin, *Nano Lett.* **5**, 1824 (2005).
- [20] N. Arjmandi, W. Van Roy, L. L., and G. Borghs, *Anal. Chem.* **84**, 8490 (2012).
- [21] K. Robards and D. Ryan, *Principles and Practice of Modern Chromatographic Methods* (Elsevier, Amsterdam, 2022).
- [22] M. Reithinger and W. Arlt, *Chem. Ing. Tech.* **83**, 83 (2011).
- [23] V. Michaud, J. Pracht, F. Schilfarth, C. Damm, B. Platzer, P. Haines, C. Harreiß, D. M. Guldi, E. Spiecker, and W. Peukert, *Nanoscale* **13**, 13116 (2021).
- [24] A. Seidel-Morgenstern, L. C. Keßler, and M. Kaspereit, *Chemical Engineering & Technology* **31**, 826 (2008).
- [25] G. V. Soni, A. Singer, Z. Yu, Y. Sun, B. McNally, and A. Meller, *Review of Scientific Instruments* **81**, 014301 (2010).
- [26] M. S. Carvalho, *Offshore Technology Conference* p. 6 (2015).
- [27] J. Foroozesh and S. Kumar, *Journal of Molecular Liquids* **316**, 113876 (2020), ISSN 0167-7322, URL <http://www.sciencedirect.com/science/article/pii/S0167732220324478>.
- [28] H. Farhadian and A. Nikvar-Hassani, *Bulletin of Engineering Geology and the Environment* **78**, 3833 (2019), ISSN 1435-9537.
- [29] N. Boon and R. V. Roij, *Molecular Physics* **109**, 1229 (2011).
- [30] P. W. P. Preuster, C. Papp, *Acc. Chem. Res.* **50**, 74 (2017).
- [31] T. Solymosi, M. Geißelbrecht, S. Mayer, M. Auer, P. Leicht, M. Terlinden, P. Malgaretti, A. Bösmann, P. Preuster, J. Harting, et al., *Science Advances* **8**, eade3262 (2022).
- [32] T. A. M. Suter, K. Smith, J. Hack, L. Rasha, Z. Rana, G. M. A. Angel, P. R. Shearing, T. S. Miller, and D. J. L. Brett, *Advanced Energy Materials* **11**, 2101025 (2021).
- [33] N. Du, C. Roy, R. Peach, M. Turnbull, S. Thiele, and C. Bock, *Chemical Reviews* **122**, 11830 (2022).
- [34] C. Hepburn, E. Adlen, J. Beddington, E. A. Carter, S. Fuss, N. Mac Dowell, J. C. Minx, P. Smith, and C. K. Williams, *Nature* **575**, 87 (2019).
- [35] B. Alberts, A. Johnson, J. Lewis, M. Raff, K. Roberts, and P. Walter, *Molecular Biology of the Cell* (Garland Science, Oxford, 2007).
- [36] R. Pethig, in *Modern Bioelectrochemistry*, edited by F. Gutmann and H. Keyzer (Springer US, Boston, MA, 1986), pp. 199–239, ISBN 978-1-4613-2105-7, URL https://doi.org/10.1007/978-1-4613-2105-7_7.
- [37] G. R. Dubyak, *Advances in Physiology Education* **28**, 143 (2004).
- [38] C. Calero, J. Faraudo, and M. Aguilera-Arzo, *Phys. Rev. E* **83**, 021908 (2011).
- [39] A. Peyser, D. Gillespie, R. Roth, and W. Nonner, *Biophysical Journal* **107**, 1841 (2014).
- [40] H. Lee, D. Segets, S. Süß, W. Peukert, S.-C. Chen, and D. Y. Pui, *Journal of Membrane Science* **524**, 682 (2017), ISSN 0376-7388.
- [41] D. V. Melnikov, Z. K. Hulings, and M. E. Gracheva, *Physical Review E* **95**, 063105 (2017).
- [42] P. Bacchin, *Membranes* **8**, 10 (2018).
- [43] A. M. Berezhkovskii, L. Dagdug, and S. M. Bezrukov, *J. Chem. Phys.* **151**, 054113 (2019).
- [44] M. Nipper and J. Dixon, *Cardiovasc. Eng. Technol.* **2**, 296 (2011).
- [45] H. Wiig and M. Swartz, *Physiol. Rev.* **92**, 1005 (2012).
- [46] A. P. Yoganathan, E. G. Cape, H.-W. Sung, F. P. Williams, and A. Jimoh, *Journal of the American College of Cardiology* **12**, 1344 (1988), ISSN 0735-1097, <https://www.onlinejacc.org/content/12/5/1344.full.pdf>, URL <https://www.onlinejacc.org/content/12/5/1344>.
- [47] K. H. Jensen, K. Berg-Sørensen, H. Bruus, N. M. Holbrook, J. Liesche, A. Schulz, M. A. Zwieniecki, and T. Bohr, *Rev. Mod. Phys.* **88**, 035007 (2016).
- [48] T. Shimmen and E. Yokota, *Current Opinion in Cell Biology* p. 68 (2004).
- [49] R. Zwanzig, *J. Phys. Chem.* **96**, 3926 (1992).
- [50] D. Reguera and J. M. Rubi, *Phys. Rev. E* **64**, 061106 (2001).
- [51] P. Kalinay and J. K. Percus, *J. Chem. Phys.* **122**, 204701 (2005).
- [52] P. Kalinay and J. K. Percus, *Phys. Rev. E* **72**, 061203 (2005).
- [53] P. Kalinay and J. K. Percus, *Phys. Rev. E* **78**, 021103 (2008).
- [54] S. Martens, G. Schmid, L. Schimansky-Geier, and P. Hänggi, *Phys. Rev. E* **83**, 051135 (2011).
- [55] G. Chacón-Acosta, I. Pineda, and L. Dagdug, *J. Chem. Phys.* **139**, 214115 (2013).
- [56] P. Malgaretti, I. Pagonabarraga, and J. Rubi, *Frontiers in Physics* **1**, 21 (2013).
- [57] P. Malgaretti, I. Pagonabarraga, and J. M. Rubi, *Phys. Rev. Lett.* **113**, 128301 (2014).
- [58] P. Malgaretti, I. Pagonabarraga, and J. M. Rubi, *Macromol. Symposia* **357**, 178 (2015).
- [59] P. Malgaretti, I. Pagonabarraga, and J. Miguel Rubi, *J. Chem. Phys.* **144**, 034901 (2016).
- [60] M. Chinappi and P. Malgaretti, *Soft Matter* **14**, 9083 (2018).
- [61] P. Malgaretti, M. Janssen, I. Pagonabarraga, and J. M. Rubi, *J. Chem. Phys.* **151**, 084902 (2019).
- [62] D. Reguera, G. Schmid, P. S. Burada, J. M. Rubi, P. Reimann, and P. Hänggi, *Phys. Rev. Lett.* **96**, 130603 (2006).
- [63] D. Reguera, A. Luque, P. S. Burada, G. Schmid, J. M. Rubi, and P. Hänggi, *Phys. Rev. Lett.* **108**, 020604 (2012).
- [64] U. Marini Bettolo Marconi, P. Malgaretti, and I. Pagonabarraga, *J. Chem. Phys.* **143**, 184501 (2015).
- [65] P. Malgaretti, I. Pagonabarraga, and J. Rubi, *Entropy* **18**, 394 (2016).

- [66] A. Puertas, P. Malgaretti, and I. Pagonabarraga, *J. Chem. Phys.* **149**, 174908 (2018).
- [67] P. Malgaretti and J. Harting, *Soft Matter* **17**, 2062 (2021).
- [68] V. Bianco and P. Malgaretti, *J. Chem. Phys.* **145**, 114904 (2016).
- [69] P. Malgaretti and G. Oshanin, *Polymers* **11**, 251 (2019).
- [70] I. V. Bodrenko, S. Salis, S. Acosta-Gutierrez, and M. Ceccarelli, *J. Chem. Phys.* **150**, 211102 (2019).
- [71] P. Malgaretti and H. Stark, *The Journal of Chemical Physics* **146**, 174901 (2017).
- [72] P. Kalinay, *Phys. Rev. E* **106**, 044126 (2022).
- [73] G. C. Antunes, P. Malgaretti, J. Harting, and S. Dietrich, *Phys. Rev. Lett.* **129**, 188003 (2022).
- [74] A. Ledesma-Durán, S. I. Hernández-Hernández, and I. Santamaría-Holek, *The Journal of Physical Chemistry C* **120**, 7810 (2016).
- [75] G. Chacón-Acosta, M. Núñez-López, and I. Pineda, *J. Chem. Phys.* **152**, 024101 (2020).
- [76] P. Malgaretti, I. Pagonabarraga, and J. Miguel Rubi, *J. Chem. Phys.* **144**, 034901 (2016).
- [77] A. M. Berezhkovskii, M. A. Pustovoit, and S. M. Bezrukov, *J. Chem. Phys.* **126**, 134706 (2007).
- [78] P. S. Burada, G. Schmid, D. Reguera, J. M. Rubi, and P. Hänggi, *Phys. Rev. E* **75**, 051111 (2007).
- [79] A. M. Berezhkovskii, L. Dagdug, and S. M. Bezrukov, *J. Chem. Phys.* **143**, 164102 (2015).
- [80] P. Kalinay and J. K. Percus, *Phys. Rev. E* **74**, 041203 (2006).
- [81] I. Pineda, J. Alvarez-Ramirez, and L. Dagdug, *J. Chem. Phys.* **137**, 174103 (2012).
- [82] A. A. García-Chung, G. Chacón-Acosta, and L. Dagdug, *J. Chem. Phys.* **142**, 064105 (2015).
- [83] S. Lifson and J. L. Jackson, *J. Chem. Phys.* **36**, 2410 (1962).
- [84] P. Reimann, C. Van den Broeck, H. Linke, P. Hänggi, J. M. Rubi, and A. Pérez-Madrid, *Phys. Rev. Lett.* **87**, 010602 (2001).
- [85] M. F. Carusela, P. Malgaretti, and J. M. Rubi, *Phys. Rev. E* **103**, 062102 (2021).